The Pennsylvania State University

The Graduate School

College of Engineering

EFFECTS OF OXYGEN TRANSPORT ON PERFORMANCE OF MICROBIAL FUEL CELLS

A Thesis in

Environmental Engineering

by

Yi Zhao

Submitted in Partial Fulfillment
of the Requirements
for the Degree of

Master of Science

August 2013

The thesis of Yi Zhao was reviewed and approved* by the following:

John M. Regan
Professor of Environmental Engineering
Thesis Advisor

Matthew M. Mench
Professor and Condra Chair of Excellence in Energy Conversion & Storage

Christopher Gorski
Assistant Professor of Civil Engineering

Peggy Johnson
Professor of Civil Engineering
Head of the Department of Civil and Environmental Engineering

*Signatures are on file in the Graduate School

ABSTRACT

Microbial fuel cells (MFCs) are a promising technology for extracting energy from pollutants in wastewater. The slow oxygen transport in the cathode of a typical air-cathode MFC is one of the limiting factors giving rise to low kinetics of the oxygen reduction reaction (ORR) in these systems. This research was aimed at studying gas-phase oxygen transport in air-cathode MFCs by the comparative performance of heliox-(21% oxygen and 79% helium, which enhances oxygen diffusivity relative) and air-supplied reactors. Identical air-cathode MFCs were operated until they all attained stable electrochemical performance. Two pairs of reactors were then switched to either air- or heliox-fed conditions, with one reactor maintain as an air-cathode control. The cathode potentials of heliox-fed MFCs significantly increased and were higher than those of air-fed reactors. At a gas flow rate of 5 L/ h, the highest peak current obtained by heliox-fed MFCs was 10 A/m^2, compared to 9.1 A/m^2 in air-fed MFCs. The maximum power density of heliox-fed reactors (1320 ± 50 mW/m^2) was 26% higher than that of air-fed systems (1050 ± 40 mW/m^2). Electrochemical impedance spectroscopy (EIS) was performed to characterize cathode and system impedances. The internal resistance of heliox-fed MFCs was 27% lower than that of air-fed reactors at a cathode potential of 0.4 V and 51% lower at 0 V. A significant decrease in diffusion resistance-the dominant component of internal resistance–was measured for heliox systems relative to air-fed reactor. Heliox-fed MFCs also had slightly better chemical oxygen demand (COD) removal efficiencies, and both gas conditions had comparable Coulombic efficiencies (CEs). Collectively, these results demonstrate that heliox improved oxygen transport to

the cathode catalyst by decreasing the diffusion resistance, without inducing negative effects associated with excessive oxygen intrusion to the MFCs.

TABLE OF CONTENTS

LIST OF FIGURES

ACKNOWLEDGEMENTS

First of all, I would like to thank my advisor, Dr. John Regan, for providing me the opportunity to pursue a graduate degree at Penn State. I can never thank enough for all of his guidance, encouragement, support and patience, which indeed made me grow up.

I would also like to express my appreciation to Dr. Matthew Mench, Dr. Christopher Gorski and Dr. Peggy Johnson for their support and serving as my committee. Especially, I wish to acknowledge Dr. Mench for his advice on my research. Also, I'm thankful to Dr. Logan for his great suggestions.

I want to thank all my labmates, especially Dr. Fang Zhang, Hiroyuki Kashima, Lijiao Ren and Dr. Hengjing Yan for their great help. I also show my thanks to Dr. Xiaoyuan Zhang for the help on EIS. I also gratefully thank the army research office, which funds me and supports my research during my graduate study.

Finally, I want to express my deep appreciation to my parents. Without their consistent love, support, generosity and encouragement, none of these would be possible. I would like to give my special thanks to my fiance Renzhong Du, for all of his help, encouragement and company. I also thank all my friends in state college, for all the joys and happiness we share together.

Yi Zhao

June, 2013

Chapter 1

Introduction

1.1 The Challenges of Energy and Wastewater Treatment

The rapid industrialization of civilizations and accompanying population explosion has caused serious energy concerns. Fossil fuels such as petroleum, coal, and natural gas have been the main energy sources for the last century, accounting for more than 80% of total energy consumption [1], and the consumption of these nonrenewable fuels increased sharply in the last half century. The total energy consumption increased from 54 quads in 1965 to 97.3 quads in 2011 in the United States alone, representing a 45% increase in just 56 years [1]. It is clear that fossil fuels cannot indefinitely sustain the global economy [2], so alternative energy sources and energy conservation measures are urgently required.

In addition to the energy crisis, the expanding industrialization and population have caused a significant increase in wastewater production. Conventional wastewater treatment technologies are energy intensive, with municipal wastewater treatment alone accounting for about 3% of the total electrical energy use of the United States [3]. Therefore, new energy-sustainable wastewater treatment techniques would help address both the energy crisis and the feasibility of sanitation in developing countries that cannot afford the energy burden of conventional approaches.

1.2 Microbial Fuel Cells for Bioenergy Production

Microbial fuel cells (MFCs) possess the potential ability of simultaneous wastewater treatment and energy generation [4], making them of great interest in environmental science and engineering in the past decade. In an MFC, organic matter is oxidized by microorganisms, some of which transfer the electrons exogeneously to an anode as a terminal electron acceptor. These electrons generate electrical current that is directly associated with the waste organics degradation.

Initial MFC designs were two-chamber systems consisting of an anode chamber, a cathode chamber, and a membrane in between the two chambers as a separation. In the anode chamber, anaerobic bacteria grow and degrade organic matter, producing electrons and protons. In the cathode chamber, the cathode is typically sparged with air to provide dissolved oxygen for the reaction of electrons with the cathode. The membrane allows charge transfer between the two chambers, while preventing excessive organics from entering the cathode chamber and dissolved oxygen from diffusing into the anode chamber, thereby keeping the anode chamber predominantly an anaerobic environment for high electricity production [2].

The high internal resistance of two-chamber MFCs limits the power generation in these systems, so single-chamber MFCs were developed to reduce internal resistance (Figure 1.1). These systems can be membraneless, which further reduces the internal resistance and makes single-chamber MFCs more practical for scale up of MFCs given the added cost of membranes. The power produced in a membraneless single-chamber MFCs with glucose was 494 ± 21 mW/m^2, while the power density was reduced to about 262 ± 10 mW/m^2 in the presence of a cation exchange membrane [2].

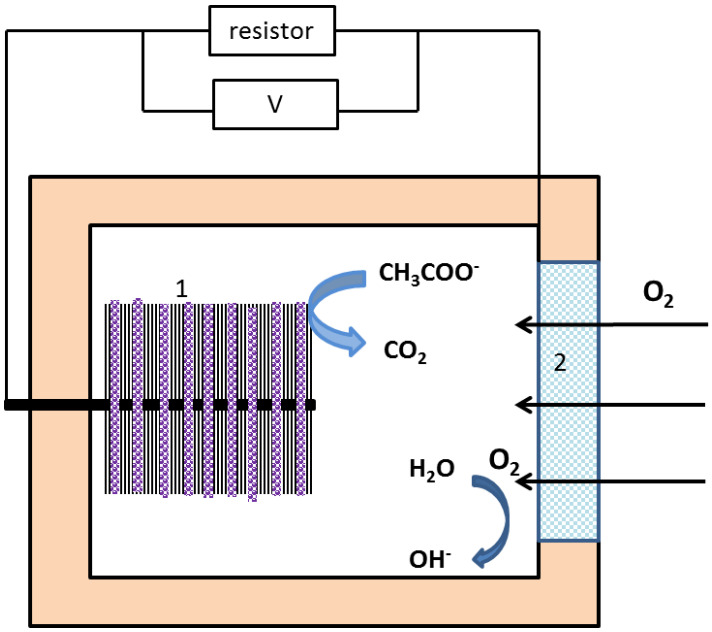

Figure 1.1. Schematic of a single-chamber microbial fuel cell. (1: brush anode electrode; 2: cathode electrode.)

1.3 Objectives

Scale up of MFCs has not been commercially realized in part due to the low power density produced by bench-scale MFCs. Though recently the power density produced by MFCs has been significantly increased, it is still more than 10 times lower than other sustainable energy technologies [5]. A common bottleneck in the development of MFCs is the slow kinetics of the oxygen reduction reaction (ORR), which is influenced by oxygen transport to the cathode [6]. Thus, this thesis research focused on the cathode constraint and the influence of oxygen transport on MFC performance.

In this study, a single-chamber cubic MFC with an extra gas feed chamber was used to investigate the effect of oxygen diffusion coefficient on the performance of MFCs. Because oxygen has a much higher diffusion coefficient in helium than in

nitrogen, it was hypothesized that sparging heliox (21% oxygen, balance helium) in the gas feed chamber would improve the oxygen transport to the cathodes compared to air-sparged cathodes, resulting in better performance of heliox MFCs.

1.4 Organization of the Thesis

This thesis is organized with a literature review in Chapter 2, materials and methods in Chapter 3, results in Chapter 4, discussion in Chapter 5, conclusions in Chapter 6, and future work in Chapter 7. Additional research I did during my Master's degree, which is not included in this thesis, was studying the mechanism of elevated baseline current generation in microbial electrolysis cells (MECs).

Chapter 2

Literature Review

2.1 Basics of Oxygen Reduction Reaction in MFCs

In MFCs, oxygen is commonly used as the electron acceptor at the cathode. The fundamental reaction occurring at the cathode catalyst in an MFC is the oxygen reduction reaction (ORR). The most frequent depiction of the ORR in MFCs is that of oxygen reacting with protons to produce water on the cathode (Eq. 2.1) [7-11]. Alternatively, the ORR has been proposed to be the reaction between protons and oxygen to produce H_2O_2 as an intermediate, which subsequently reduces to water (Eqs. 2.2 a and b)[12]. However, Popat *et al.* [13] found that when they replaced Nafion binder (efficient in cation transport) with an anion-conducting binder, the Nernstian concentration losses due to an increase of pH (60 mV/pH unit) can be partially overcome. This suggested involvement of an anionic moving, and they concluded that the ORR on the cathode is that of oxygen and water reacting to produce hydroxyl (Eq. 2.3).

$$O_2 + 4H^+ + 4e^- \rightarrow 2H_2O \qquad (2.1)$$

$$O_2 + 2H^+ + 2e^- \rightarrow H_2O_2 \qquad (2.2a)$$

$$H_2O_2 + 2H^+ + 2e^- \rightarrow 2H_2O \qquad (2.2b)$$

$$O_2 + 2H_2O + 4e^- \rightarrow 4OH^- \qquad (2.3)$$

2.2 Influence of Oxygen on ORR in MFCs

In MFCs systems using oxygen as the electron acceptor, oxygen transport to the cathode has been considered a limiting factor for the low kinetics of the ORR [6]. There have been studies on the influence of oxygen concentration on MFC performance [11, 14, 15]. Oh *et al.* [11] tested the effect of dissolved oxygen (DO) on the power generation of two-chamber MFCs under unsteady-state and steady-state conditions. In the unsteady-state test, the cathode chamber was filled with air-saturated water. In the steady-state test, the cathode chamber was continuously sparged with mixture gas (nitrogen and oxygen) with different concentrations of oxygen to achieve a DO concentration in the range of 0-37.7 mg/L. They found that the power generation increased with DO in the low DO region and saturated at high DO concentrations, approximately above 4 mg/L. Juang *et al.* [14] also studied the influence of oxygen concentration by providing oxygen using two different means, with one MFC supplied oxygen from mechanical aeration in the cathodic chamber and the other obtaining oxygen from algae growing in the cathode. They found that the mechanical aeration MFCs had better performance, possibly due to the higher oxygen concentration. In a similar work done by Cha *et al.* in 2010, MFCs were submerged in the aeration tank for wastewater treatment [15]. Their results showed that the voltages produced by the MFCs directly responded to changes in air flow rate of the blower. When the air flow rates increased from 0 L/min to 10 L/min, the DO concentration slightly raised or remained nearly constant, but the cell voltage increased by 4 to 5 times. When different cathode materials were used in this experiment, such as carbon cloth and graphite felt, the trends of change in voltage with aerated flow rate were the same. This indicated that the concentration of oxygen in the bulk solution was not a

key limiting factor for the ORR at the cathodes. The authors proposed that the rate of oxygen transfer into the cathode depended on the mixing intensity but not bulk oxygen concentration, but there have been few studies on the influence of oxygen transport on the performance of MFCs.

2.3 Attempts to Improve ORR on Cathodes

The main attempts to improve the ORR on cathodes have focused on the development of new cathode structures and the application of new materials and cathode catalysts. These approaches can significantly affect oxygen transfer to the cathode and crossover to the anode, therefore influencing MFC performance beyond just the ORR. There have been numerous studies on these directions [16-23].

2.3.1 Improvement of Cathode Structure

The main emphasis for improving cathode structure has been on the inclusion of gas diffusion layers (DLs). Cheng *et al*. [16] showed an improvement of single-chamber MFC performance with the application of successive coatings of polytetrafluoroethylene (PTFE) layers on a carbon base cathode. An optimal condition was obtained with four DLs, which resulted in a 171% increase in the CE and a 42% increase in the maximum power density, as compared with a carbon base cathode without PTFE coating. The authors attributed the enhanced performance to the improvement of the three-phase interface for oxygen reduction, as well as the prevention of water loss and consequent flooding at the cathode which helped the oxygen transport.

Similarly, Santoro *et al.* [17] compared the performance of single-chamber MFCs with different cathode structures. In their study, three types of novel cathode structures

were prepared, including two-layer (gas diffusion layer (GDL) and catalyst layer (CL)), three-layer (GDL, micro porous layer (MPL), and CL), and multi-layer (GDL, CL, carbon-based layer (CBL), and hydrophobic layers) structures (Figure 2.1). The results showed that the three-layer cathode had the lowest ohmic resistance (30 ohm compared with 91 ohm for the single-layer cathode and 60 ohm for the multi-layer cathode) and the highest open circuit potential (OCP), and therefore gave the highest power density of about 500 mW/m^2. It was suggested that the MPL between the GDL and CL in the three-layer cathode played an essential role in improving the performance of the MFC by preventing biofilm penetration into the cathode, reducing water loss, and facilitating the ORR. As a result, highly enhanced overall electrical conduction, power generation, and organic substrate removal were achieved.

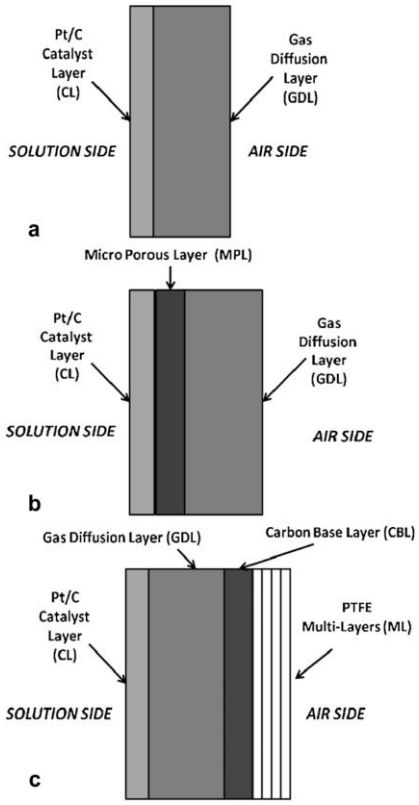

Figure 2.1. The diagrams of (a) two-layer (2L), (b) three-layer (3L), and (c) multiple-layer (ML) cathode configurations [17].

2.3.2 Utilization of New Cathode Materials

Another strategy to improve cathode performance involves the use of new cathode materials and catalysts. Zhang *et al*. [18] found that stainless steel (SS) mesh cathodes with poly(dimethylsiloxane)(PDMS) and carbon black DLs had better performance than SS with PDMS alone because of higher oxygen transfer coefficients. The carbon black created a microporous hydrophobic layer to improve oxygen transport.

An air cathode comprised of activated carbon (AC) with a Ni mesh current collecter was developed by Zhang *et al.* as another alternative to the more typical platinum-carbon cloth air cathode [19]. The AC cathode had a maximum power density of 1220 mW/m^2, even higher than that produced by the Pt-catalyzed carbon cloth cathode (1060 mW/m^2). The large surface area of AC provides more interface for the ORR, leading to better performance. Also, due to the much lower price of AC and Ni mesh, this novel cathode is a promising candidate for MFC scale up.

2.3.3 Alternative Cathode Catalysts

Catalysts are often necessary in MFCs for the purpose of overcoming the high over-potential barrier of the ORR. Platinum is a commonly used catalyst in MFCs due to its chemical stability and high activity, but it has a prohibitive disadvantage of high cost [20]. In the past years, many efforts have been devoted to identifying and developing alternative effective and inexpensive catalysts.

The cathodic performance of MFCs with Fe_2O_3 nano-powder, Mn_2O_3 nano-powder, and carbon black powder were compared by measuring their ORR catalytic activity [21]. The results indicated that Mn_2O_3 is the most promising alternate catalyst material for the replacement of Pt [21]. Liu *et al.* [24] used nano-structured manganese oxide (MnO_x) as a cathodic catalyst to enhance oxygen reduction in MFCs, and reached a maximum power density 773 mw/m^3, which was close to the maximum power density produced by a Pt cathode. The schematic pathways of oxygen reduction on the MnO_x nanorods are shown in Figure 2.2.

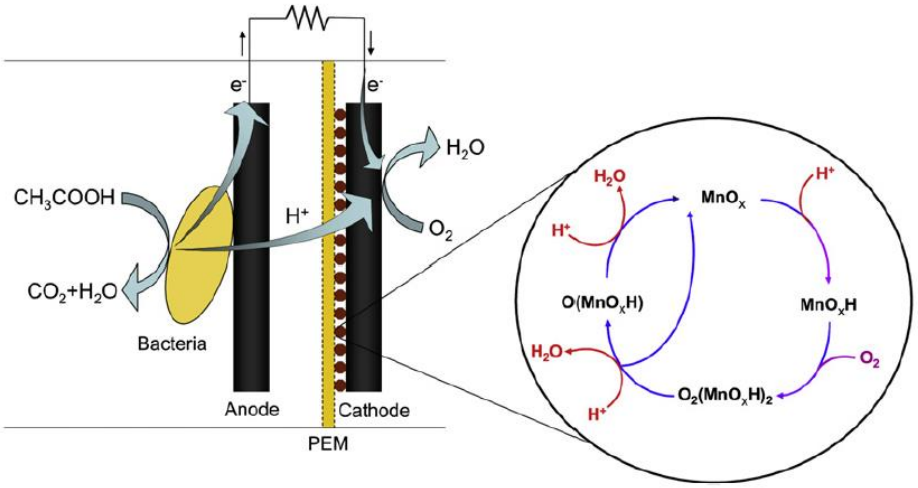

Figure 2.2. Schematic pathways of oxygen reduction on the MnO_x nanorods in a single-chamber air-cathode MFC (Source: [24]).

AC and activated graphite are used broadly as catalysts in industry due to their large surface area, low cost, and chemical stability. Also, AC has oxygen and nitrogen groups on its surface, so nitric acid activation of graphite granules has been used to improve the ORR in MFCs. The OCP can reach 1050 mV when using activated graphite granules, which is one of the highest OCPs reported so far [22]. A big improvement of

ORR was observed with activated granules compared to untreated granules [22]. The increase of surface area combined with oxygenated groups, such as nitrogen functional groups [25], are thought to result in this improvement. In electrochemical tests, two less-expensive metal catalysts, Co-tetra-methyl phenylporphyrin (CoTMPP) and iron phthalocyanine (FePc), have been shown to produce comparable performance with Pt-coated cathodes when the current is above 0.2 mA/cm^2 in air-saturated conditions [23].

2.3.4 Improvement of Oxygen Diffusion Coefficient by Heliox

Most research on the improvement of MFC cathode performance has focused on the application of new materials, catalysts, or structures. Ameliorating oxygen diffusion constraints through the use of heliox offers a complementary research method to explore and address these cathode constraints.

Heliox is a mixture of 21% oxygen and 79% helium. The first use of heliox in clinical applications was in 1935 as a therapy for asthma exacerbations [26]. It is used broadly in medicine nowadays because it is a low density gas that improves oxygen transport relative to air. Also, it prevents the transition from laminar to turbulent flow, giving less resistance and lower particle drug loss [26]. Lee *et al.* found that spirometry values of 80 adult asthmatics were improved significantly with heliox-driven albuterol nebulization compared to air as the carrier gas [27]. Heliox can also be used to enhance breathing environments for divers [28], especially for deep diving.

Though there have not been any publications on the use of heliox to study MFCs, there have been many studies on the utilization of heliox in proton exchange membrane fuel cells [29, 30]. Herrera *et al.* [29] analyzed the anode and cathode overpotentials in a

multi-component gas system (oxygen, air, and heliox), which enabled the development of a model of the gas transport. Also, Srouji *et al.* [30] studied the performance and mass transport of a polymer electrolyte fuel cell with an open metallic element flow field architecture compared to a conventional parallel channel/land fuel cell. They found that a heliox mixture at the cathode resulted in improved mass transport, but no oxygen gas phase transport limitation at high current density was observed.

The ORR at the cathode surface of MFCs is a slow process in part due to the low diffusion coefficient of oxygen [6], and addressing this important limiting factor is necessary for the improvement of power production and practical use of MFCs. Therefore, accelerating oxygen transport by optimizing its diffusivity could be used to study cathode configurations that improve performance of MFCs. Owing to the higher oxygen diffusivity (compared to air) and the biological inertness [28] of helium, heliox offers an experimental approach to accelerate gas-phase oxygen transport and evaluate the effect on the ORR and overall power generation of MFCs.

Chapter 3

Materials and Methods

3.1 Reactor and System Configuration

The reactors used in these experiments were single-chamber cubic-shaped MFCs (length 4 cm, diameter 3 cm, volume 28 mL) [31]. In order to sparge heliox (21% oxygen, balance of helium) or air continuously and keep the gas flow rate steady, one extra chamber (length 2 cm, diameter 3 cm, volume 14 mL) was added to the MFCs. In addition, a standard cubic MFC without this added chamber was used as a control. (Figure 3.1).

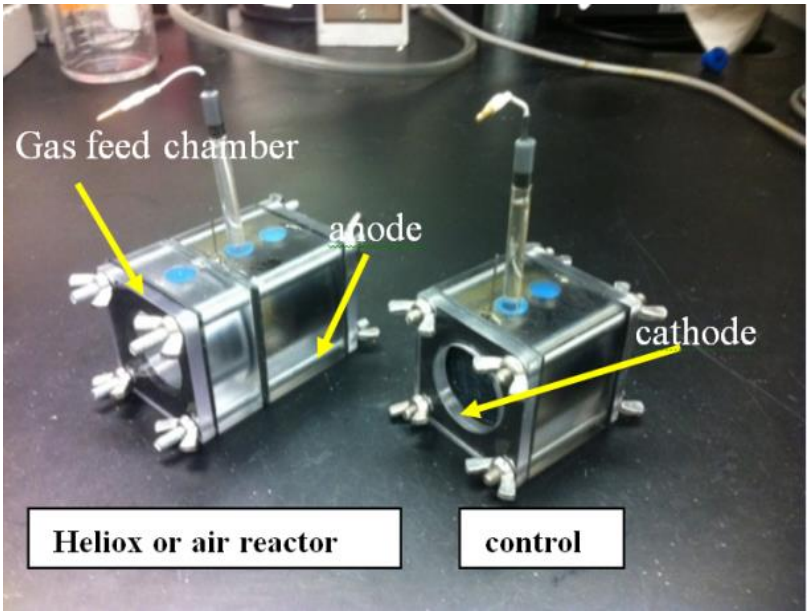

Figure 3.1.Reactor configurations for continuous gas sparging and control MFCs.

Graphite fiber brush anodes with a length of 25 mm and diameter 25 mm (fiber type PANEX 33 160 K, ZOLTEK) were heat treated at 450 °C for 30 min [32, 33]. The support material of cathodes was carbon cloth (30% Teflon treatment, CC40WP30, Fuel Cell Earth, USA). The gas-facing side was coated with a carbon base layer (a mixture of carbon black and 40% polytetrafluoroethylene [PTFE]) and four PTFE layers, while the solution-facing side was a platinum and carbon catalyst layer(0.5 mg Pt/cm^2 of cathode surface area) [16](Figure 3.2). The electrodes were connected to an external circuit by titanium wires (0.32 mm diameter). Also, an Ag/AgCl reference electrode (RE-5B, BASi, +211 mV vs. standard hydrogen electrode, SHE) was placed in the MFC chamber between the end of the anode and the cathode.

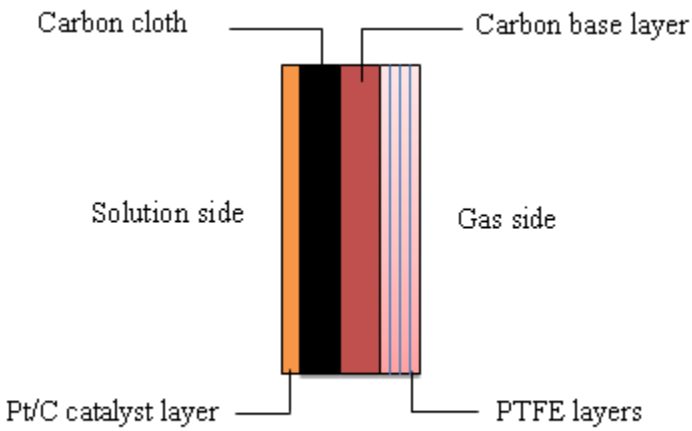

Figure 3.2.The structure of cathode

For systems with gas sparging across the cathode, heliox or air was delivered from gas cylinders and passed through a desiccant to remove moisture and maintain the same relative humidity (1%). Then the dried gas went through a flow meter to the extra 2-cm chamber, which had a needle to vent the sparged gas (Figure 3.3).

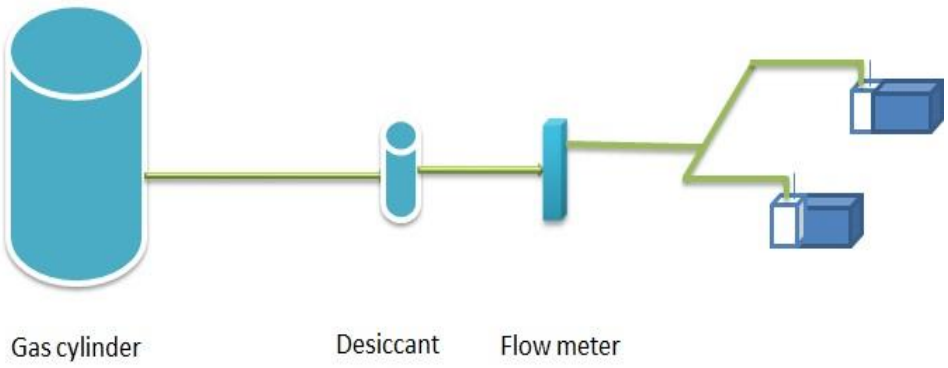

Figure 3.3. The schematic of the experimental system for sparged cathodes chambers.

3.2 Reactor Operation

All reactors were inoculated with effluent from an existing acetate-fed MFC. The feed medium contained 1 g/L sodium acetate, 10 mL/L minerals, and 10 mL/L vitamins in 50 mM phosphate buffer solution (PBS; Na_2HPO_4 4.58 g/L, $NaH_2PO_4 \cdot H_2O$ 2.45 g/L; NH_4Cl0.31g/L, KCl 0.13 g/L) [34]. The conductivity of the medium was 7.55±0.08mS/cm, and the pH was 7.08±0.01. The reactors were fed in batch mode in a 30°C room.

The reactors were started up with 1000 Ω external resistance and typical air cathodes (i.e., without the extra chamber for gas sparging), as it has been previously shown that high resistances accelerate startup [35]. After the cell voltages stabilized, the external resistances were changed from 1000 Ω to 10 Ω, and the MFCs were kept running for three additional cycles to establish consistent performance among all reactors. Then the reactors were operated under different gas conditions: the control reactor continued to be operated as a typical air-cathode MFC, and two pairs of duplicate reactors were switched to identical continuous-flow conditions of either heliox or air at 5 L/h per reactor for two cycles and then 2 L/h per reactor for three cycles.

3.3 Measurements and Calculations

Voltage (E_{cell}) across an external resistance (R_{ext}) was measured by a data acquisition system (Keithley 2700) at a 10-minute interval. The overall performance of the MFCs was evaluated based on current and power output. Current density (I) based on the cathode area (A_c) was calculated by Ohm's law ($I=E_{cell}/(R_{ext}A_c)$). Power density (P) was calculated as $P=E_{cell}^2/(R_{ext}A_c)$ [9]. Soluble COD (sCOD) was measured with the standard method (HACH COD high range kit, 20-1500 mg/L) [36]. Coulombic efficiencies (CEs) were calculated based on COD removal and current generation as follows [9]:

$$CE = \frac{M \int_0^t Idt}{FbV_{an}\Delta COD}$$

Polarization and power density data were obtained by using different external resistances (1000 ohm, 500 ohm, 200 ohm, 150 ohm, 100 ohm, 75 ohm, 50 ohm, and 10 ohm, sequentially) at 20-minute intervals in one single cycle. The gas composition was analyzed by gas chromatography (GC; model 310C for measurement of O_2, N_2, He; SRI Instruments) using a gastight syringe (250 µL, Hamilton Sample lock Syringe).

Linear sweep voltammetry (LSV) and electrochemical impedance spectroscopy (EIS) were performed with a potentiostat (BioLogic VMP3) to electrochemically characterize the cathodes. In these tests, the cathodes were set as the working electrodes, while the anodes were used as the counter electrodes and Ag/AgCl electrodes as the references. EIS was used to characterize the system internal resistance and the impedance contributions of the cathodes [37, 38]. The frequency range was from 100 kHz to 1 mHz [37] with a sinusoidal perturbation of 14.2 mV (root mean squared) amplitude and the

cathodes potentiostatically maintained at 0 V and 0.4 V versus standard hydrogen electrode (SHE). Cathode impedance spectra were fitted to an equivalent circuit (Figure 3.4) using EC-Lab software to obtain the charge transfer resistance (R_{ct}), diffusion resistance (R_d), and solution resistance (R_s) [33]. For LSV tests, MFCs were run under open circuit condition for 20 min, and then the cathodes were equilibrated to 0.5 V for half an hour. The scan range of LSV was 0.5 V to 0.2 V, with a scan rate of 1 mV/s.

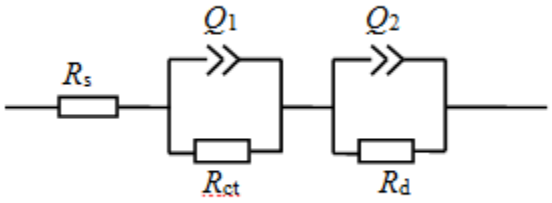

Figure 3.4. Equivalent circuit for cathode EIS

Chapter 4

Results

4.1 Electricity Generation by the Heliox- and Air-Sparged MFCs

The MFCs produced consistent and reproducible currents under the same 1000 ohm acclimation conditions (Figure 4.1), with good agreement between duplicate reactors. The peak current densities of MFCs separated after they were changed to different gas conditions, with heliox-fed cathodes producing the highest current densities and air-fed cathodes producing the lowest (Figure 4.1). At a gas flow rate of 5 L/h, the peak current density of heliox MFCs reached 10 A/m^2, while that of air-fed MFCs was 9.1 A/m^2. When the gas flux was decreased from 5 L/h to 2 L/h, the maximum current density of heliox-fed MFCs was 9.9 A/m^2, compared to 8.7 A/m^2 in air-fed MFCs. So the current density difference between heliox- and air-fed MFCs increased to 1.2 A/m^2, with the all the reactors remaining constant in the first two cycles after the gas flow rate was reduced, but one of air-fed systems and one of heliox-fed MFCs showing reducing trends of electricity generation in cycle 3.

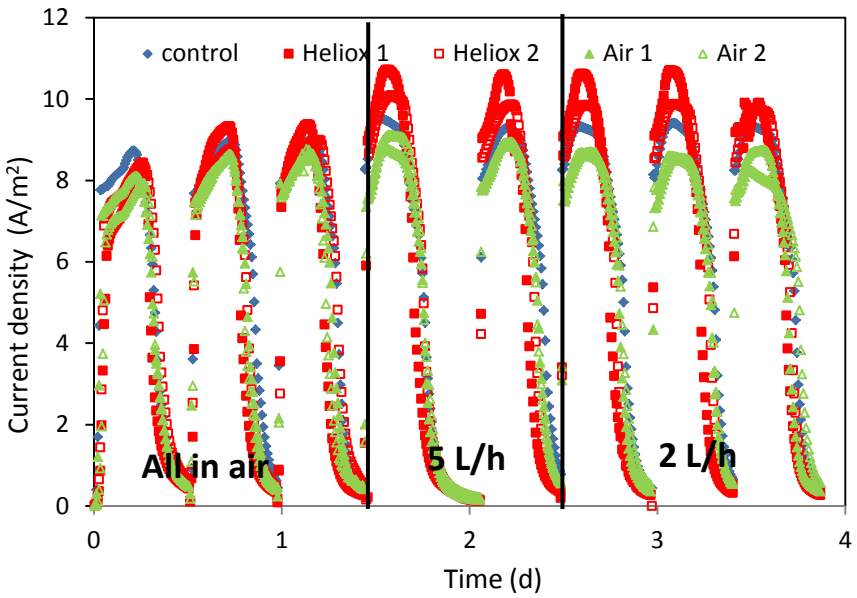

Figure 4.1. Current generated by MFCs under different air and heliox flow rate

The cathode potentials of the heliox MFCs improved after they were changed from the open air condition to the heliox-sparged configuration, increasing from -0.265 V to -0.245 V (vs Ag/AgCl) at the time of peak current (Figure 4.2(A)). However, the cathode potentials of the air-fed reactors reduced slightly after imposing this operational change. The anode potentials of air-fed MFCs and the control reactor were identical; the anode potentials of the heliox MFCs increased very slightly (Figure 4.2(B)). Therefore, the change of cathode potential due to different gas sparging conditions resulted in the different MFC performances.

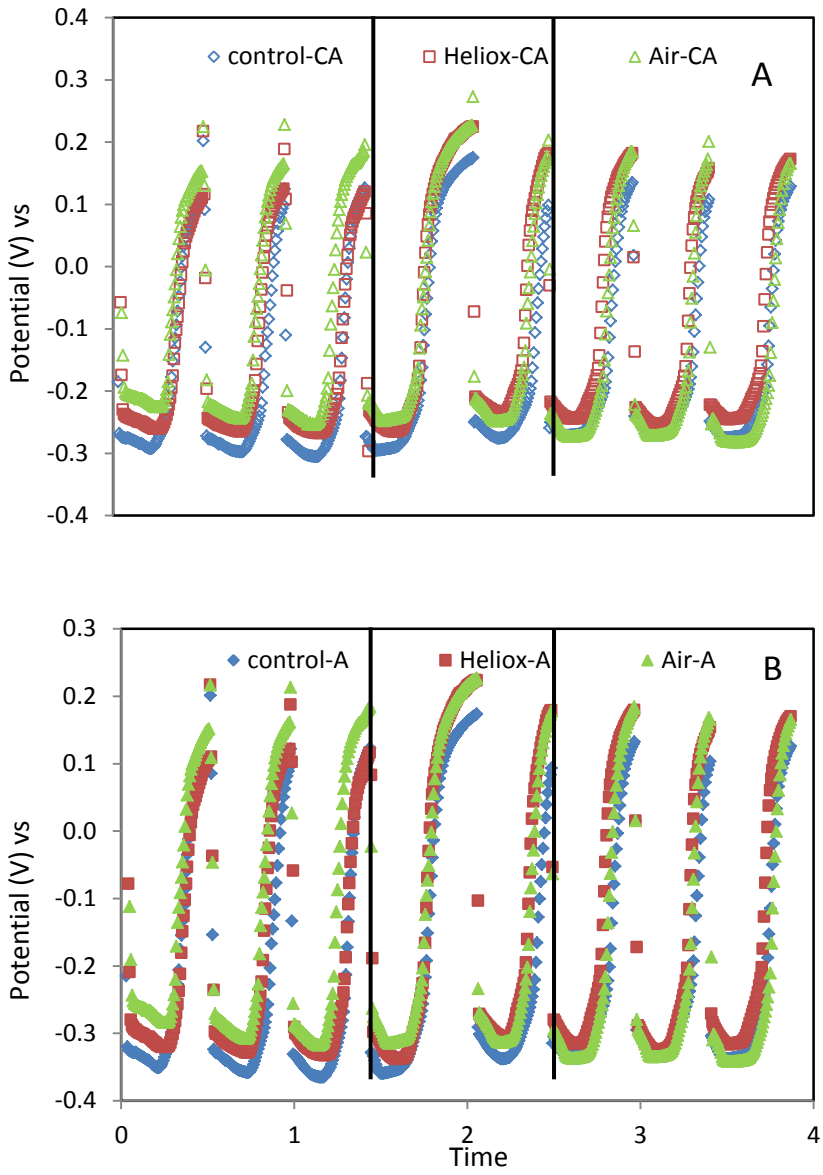

Figure 4.2. (A) Cathode potentials and (B) anode potentials for the different cathode treatment.

4.2 Power Production

The polarization tests were performed after the duplicated MFCs had identical and consistent voltages under different gas conditions. The maximum power density ($1320 \pm 50 mW/m^2$) was obtained by MFCs with heliox-supplied cathodes, while the air-

fed MFCs showed the lowest maximum power of 1050 ± 40 mW/m^2 (Figure 4.3(A)). All MFCs attained their maximum power density with an external resistance of 75 ohm. The power densities for all treatments were similar at high external resistances, with the differences emerging at the lower external resistances and associated increased oxygen demand at the cathode.

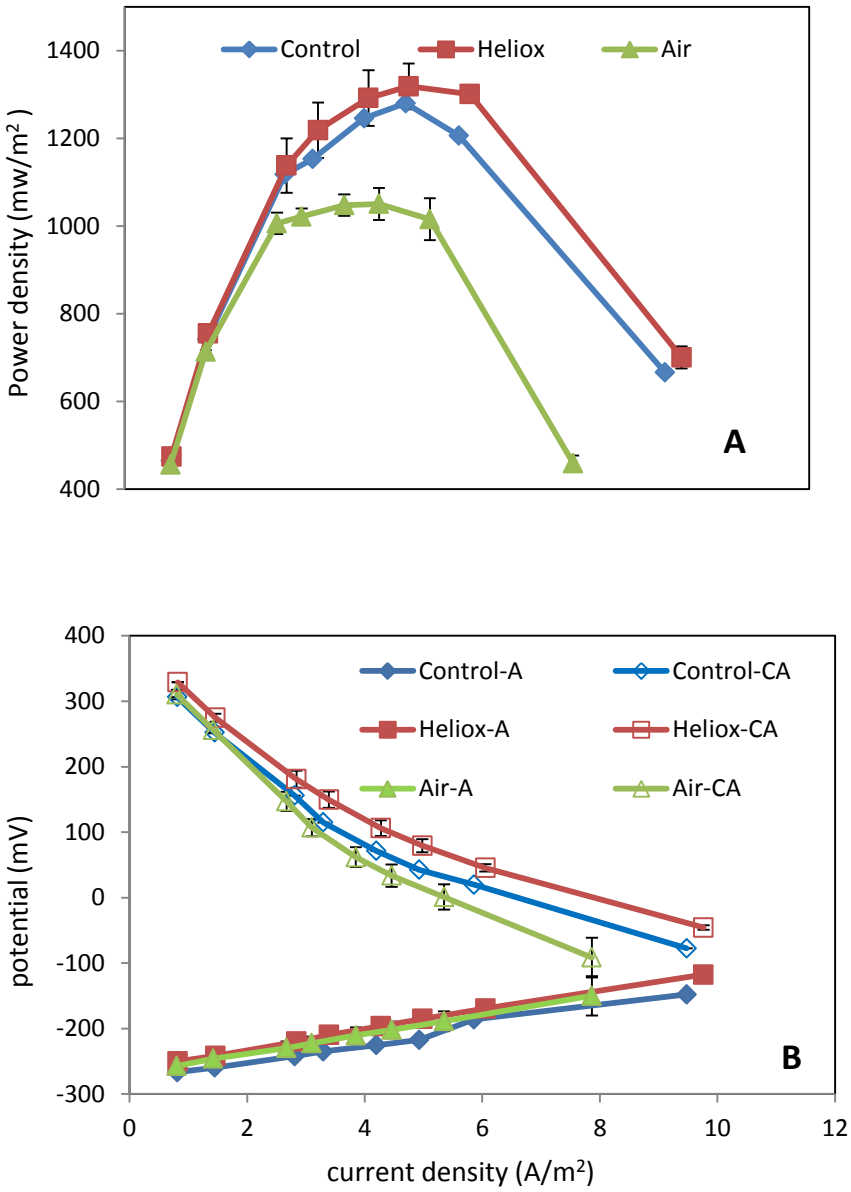

Figure 4.3. (A) Power density curves and (B) polarization curves.

The anode potentials of all MFCs were similar across the range of current densities during the polarization tests, with only slightly higher anode potential of heliox-fed MFCs observed (Figure 4.3(B)). However, noticeable difference was observed from cathode potentials with low external resistances. Heliox-fed MFCs obtained more positive cathode potentials compared to air-fed MFCs. The heliox-fed cathode potential ranged from 329.1 ± 0.3 mV to -45.8 ± 3.4 mV when the external resistance was reduced from 1000 ohm to 10 ohm, while air-fed MFCs cathode potentials were in the range of 310.4 ± 7.4 mV to -91.5± 30 mV (Figure 4.3(B)).

4.3 Coulombic Efficiency (CE) and sCOD Removal

The CEs from heliox- and air-fed MFCs were similar throughout the experiments (Figure 4.4). The average CE of heliox MFCs changed from 58% in standard air-cathode format to 65% with 5 L/h heliox and 63% with 2 L/h heliox. For the air-fed reactors, the average CE improved from 58% in ambient air conditions to 66% 5 L/h air and 63% with 2 L/h air. The highest CEs of heliox and air MFCs, achieved in the first cycle after which they were switched to continuous gas flow, were both 70%. Because the CEs of heliox and air MFCs were similar before and after they were changed to different gases, the different oxygen diffusion coefficients in heliox and air did not significantly influence the CEs. The COD removal was always above 90% for all reactor conditions (Figure 4.5), with no differences or variance of COD removal efficiency throughout the experiments.

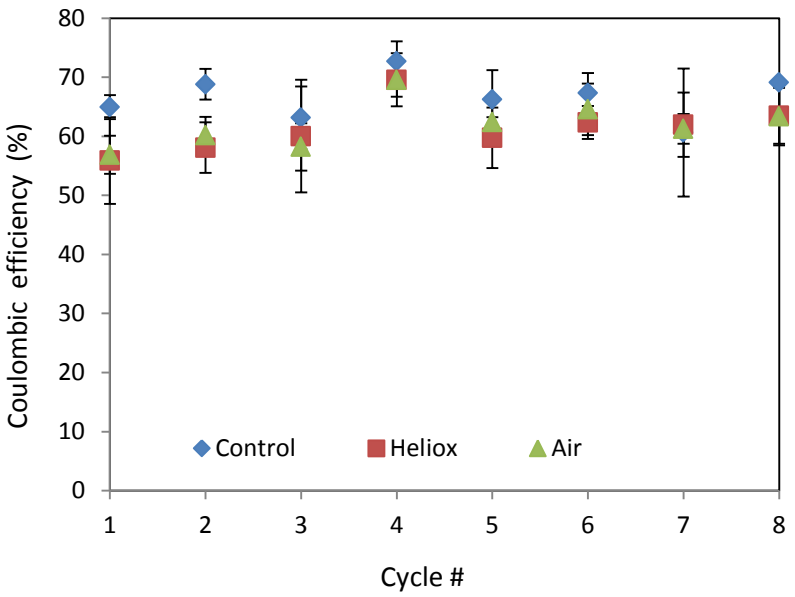

Figure 4.4.Coulombic efficiencies of MFCs

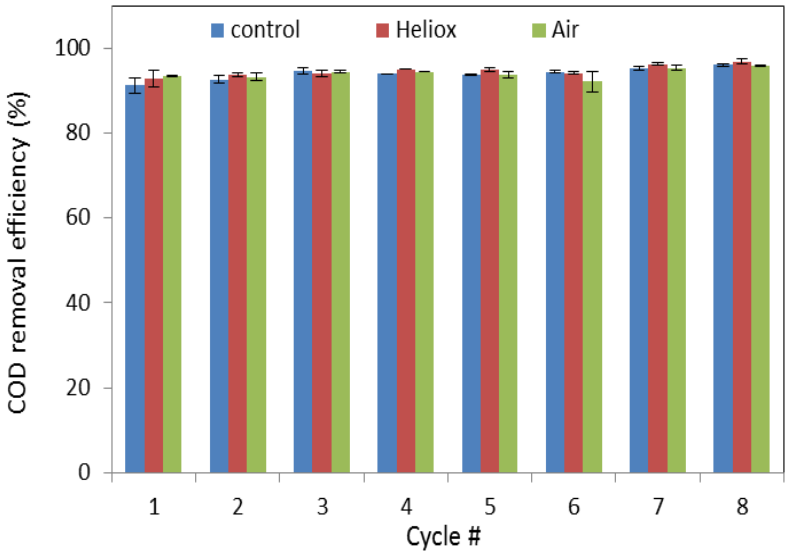

Figure 4.5.COD removal efficiencies

4.4 Electrochemical Characterization

LSV was conducted to identify the cathode overpotential performance for the reactors acclimated to different cathode gas treatments. LSV tests showed that cathodic current densities of all conditions were almost identical when the potential was higher

than 0.45 V (Figure 4.6). However, their current densities separated at lower cathode potentials, with the heliox systems showing the lowest overpotential. The current density reached 17.7 A/m^2 for the heliox cathodes at the lowest scanned potential, whereas the highest cathodic current density of the air-sparged cathodes was -9.3 A/m^2 (Figure 4.6). The LSV results indicated that heliox-supplied cathodes had much better performance than the air-supplied cathode.

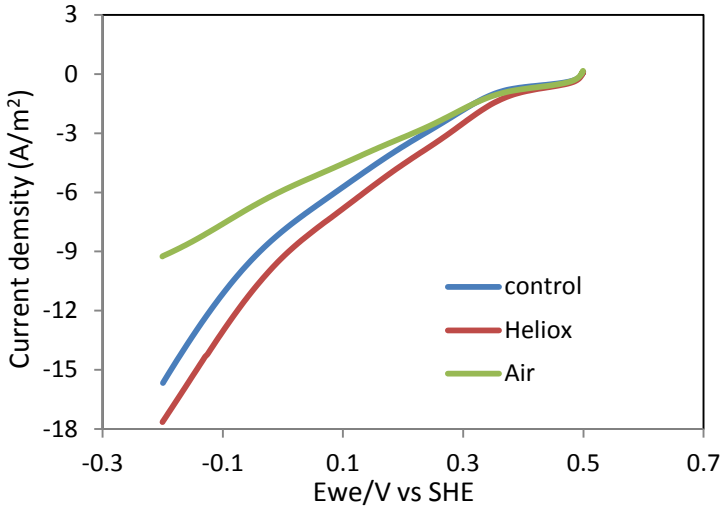

Figure 4.6.LSV of used cathodes under different gas condition

EIS was conducted at different cathode potentials of 0.4 V and 0 V (vs SHE). The spectra were fitted to an equivalent circuit (Figure 3.4) to distinguish the individual components of the cathode internal resistances. Total impedance increased with the higher set potential. The solution resistances (R_S) were similar because of the same cell configurations and solutions. At potentials of 0.4 V and 0 V, the cathodes sparged with 0.2 L/h air had the highest impedance of air-fed cathodes, as indicated by the largest diameter of semi-circle (Figure 4.7 and Figure 4.8). The cathode EIS spectra of control

and heliox reactors were close, though the impedance differences between them and with the air-supplied cathodes became more pronounced at 0 V potential.

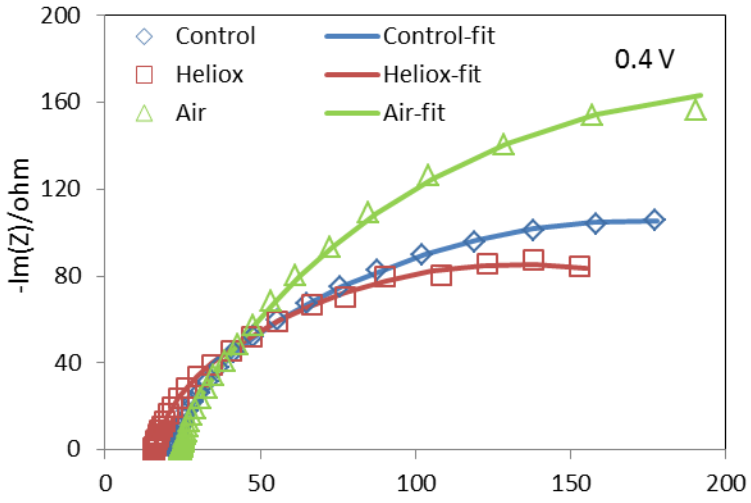

Figure 4.7.Nyquist plots of EIS spectra at cathode potentials of 0.4 V.

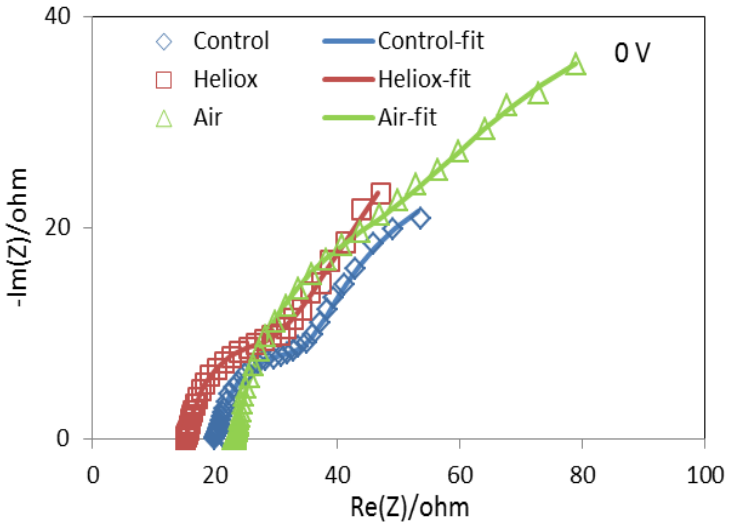

Figure 4.8. Nyquist plots of EIS spectra at cathode potentials of 0 V.

The R_d was always the dominant component for cathode impedance at both potentials of 0.4 V and 0 V (Figure 4.9). All the reactors had similar R_{ct} and R_s of

cathodes, but their R_d were very different (Figure 4.9). R_d of the heliox-fed cathode was 249 ohm, which was the lowest one compared with 308 ohm of air-fed MFC and 261 ohm of controls at 0.4 V (Figure 4.8 A). The cathodic R_d of heliox-fed, control, and air-fed MFCs at 0 V were 41 ohm, 60 ohm, and 126 ohm, respectively. The total resistance (R_t) of heliox-fed MFCs was 27% lower than that of air-fed reactors at a cathode potential of 0.4 V and 51% lower at 0 V.

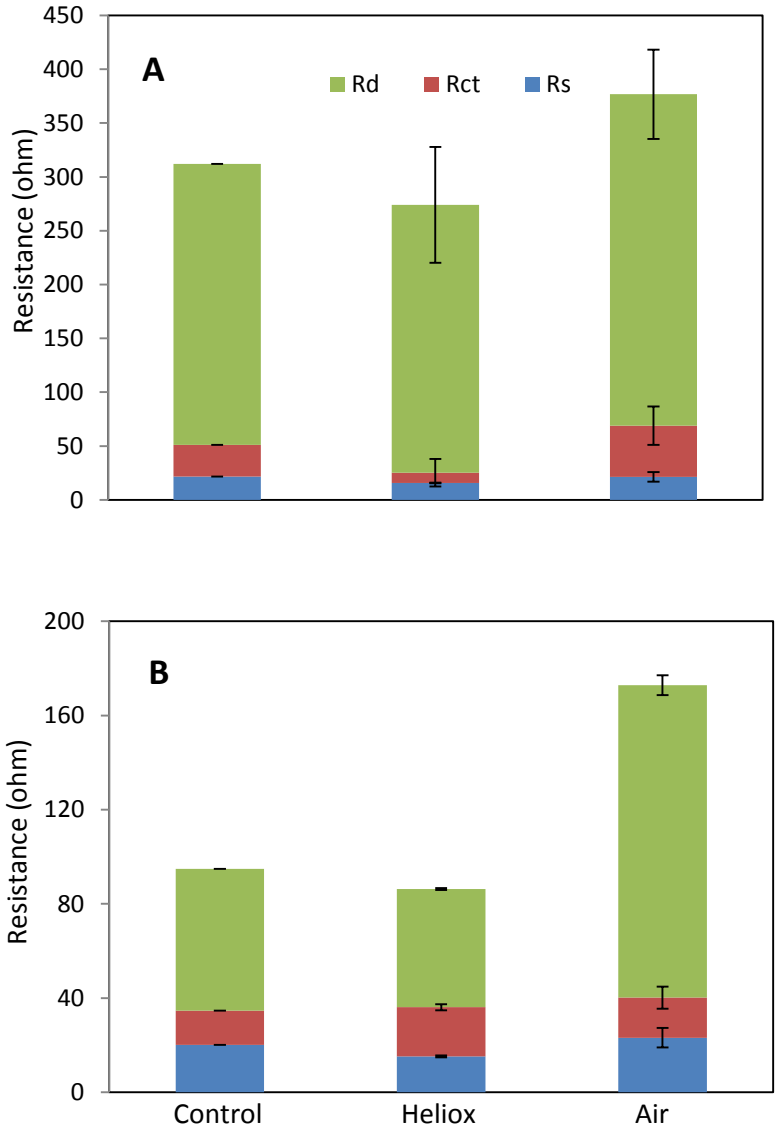

Figure 4.9.Component analysis of EIS spectra at cathode potentials of (A) 0.4 V, (B) 0 V.

4.5 Gas Composition

To ensure that the better performance of heliox reactors was not due to different oxygen percentages in the sparged chambers, the gas composition was measured at the peak current point and before the maximum current density was achieved. The oxygen percentages in gas-fed chambers of heliox and air MFCs were always approximately 21%. Therefore, the different performances of MFCs were not due to the concentration of oxygen in the chambers.

Chapter 5

Discussion

5.1 The Effects of Oxygen Diffusion on Electricity Generation

The peak current density of the heliox reactors was 10 A/m^2 with a 10 ohm external resistance, while that of air-fed cathode MFCs was 9.1 A/m^2. The current density of air-sparged MFCs was reduced when the flux decreased from 5 L/h to 2 L/h, but heliox-fed MFCs showed constant electricity production. This result indicated that the heliox improved oxygen transport, helping system reach the oxygen demand for the ORR even at low flow rate. The maximum power density of the heliox MFCs was 1320 ± 50 mW/m^2 at 75 ohm, which was 26% higher than the air-fed MFCs in this study. The maximum power density of control was about 1280 mW/m^2, which was similar to that obtained by Wei *et al.* [39], the configuration of MFCs in whose study was the same as the control system in this study. These results indicated that heliox reactors had better performance than typical air-cathode MFCs.

The diffusion coefficient of oxygen in heliox was 0.42 cm^2/s (270 Kpa$_{abs}$, 80 °C), compared to 0.11 cm^2/s in air (270 KPa$_{abs}$, 80 °C) [29]. These values can be converted to the pressure and temperature conditions in the MFC experiments using the following equation [40]:

$$D_{ca(P_p,T_T)} \cong D_{ca}\frac{P}{P_p}\left(\frac{T_T}{T}\right)^{1.75} \quad (5.1)$$

Where D_{ca} is diffusion coefficient of C in air or gas, P = pressure, and T = temperature in degree Kelvin. This results in a diffusion coefficient for oxygen of 0.86 cm^2/s in heliox,

compared to only 0.23 cm^2/s in air (101 KPa_{abs}, 30 °C). Therefore, the diffusion coefficient of oxygen in helium is 3.7 times of that of oxygen in nitrogen. The better oxygen transport to the catalyst layer due to the higher oxygen diffusion coefficient in helium might be the reason for better performance of heliox-fed MFCs.

The polarization data (Figure 4.3) show that although the faster oxygen intrusion in the heliox systems had a slightly negative effect on the anode performance, its positive impact on cathode performance outweighed this and resulted in an overall better performance with heliox cathodes.

The power generation of air-fed MFCs was lower than that obtained from the control (Figure 4.3), which might be caused by a high relative humidity (RH) in the gas chamber. Although moisture in the sparge gas was removed by desiccant before the flow meter and gas chamber, there was still observable water accumulated in the extra chamber, presumably due to the oxygen reduction reaction. The high viscosity of water made it difficult to be exhausted from the chamber through the needle. Notable water was observed in gas chambers at the end of most cycles.

5.2 The Effects of Oxygen Diffusion on Internal Resistances

EIS results showed that the cathodes of heliox MFCs had much lower internal resistance than the air MFCs at cathode potentials of 0.4 and 0 V. According to Ohm's Law, the slope of a cathode LSV curve (Figure 4.6) provides an estimate of the total internal resistance (R_t) of the cathodes. The results of LSV were consistent with the EIS data.

The diffusion resistance was the largest contributor to the impedance for all MFCs, including the heliox-fed systems. The cathodic R_d of heliox MFCs was always much lower than R_d of the air MFC cathodes. There were not big changes on the other two components of the resistances (R_s and R_{ct}), which would be expected for R_s given that all systems had the same medium and spacing between reference electrode and cathode. Therefore, the higher oxygen diffusion coefficient in heliox could largely reduce R_t of the cathode, mainly by decreasing R_d. The influence of oxygen transport was more significant at the lower cathode potential, and the different oxygen diffusion coefficients did not significantly affect R_{ct}.

5.3 The effects of oxygen diffusion on Coulombic Efficiency (CE) and sCOD Removal

The COD removal efficiency of heliox reactors was slightly higher than that of air cathode MFCs. The most likely reason was that better oxygen transport in helium raised the dissolved oxygen concentration in electrolyte, resulting in higher substrate utilization rate for biomass growth.

The CEs of heliox and air MFCs obtained in this experiment were similar, which were 62.6% (heliox) and 63.1% (air) under 2 L/h gas conditions, 64.6% (heliox) and 66% (air) under 5 L/h gas flow rate. Though the peak current of heliox reactor was higher than air-fed one, but the faster drop of current of heliox MFCs might be the reason for similar CEs.

Chapter 6

Conclusions

In air-cathode MFCs systems, the slow transport of oxygen to the cathode has been considered a limiting factor for the ORR. In this study, we therefore provided heliox gas to the cathode of single-chamber cubic MFCs to improve oxygen diffusion, comparing their performance with that of air-cathode MFCs to determine whether gas-phase oxygen transport did constrain system performance. The results of this study showed the following:

1. The maximum power density of heliox-fed MFCs were 26% higher than those of air-fed MFCs. Also, the current density of heliox-fed MFCs was 0.9 A/m^2 and 1.2 A/m^2 higher comparing with maximum current density of air-fed MFCs at 5 L/h and 2 L/h respectively. Although the faster oxygen transport in the heliox systems had a slightly negative effect on the anode performance, as seen in slightly higher anode potentials in polarization curves, its positive impact on cathode performance outweighed this and resulted in an overall higher power production.
2. Heliox-fed cathodes had much lower R_t than air-fed cathodes due to a much lower R_d associated with the better diffusivity of oxygen in helium.
3. The COD removal efficiencies of all the reactors were above 90%, among which heliox-fed MFCs had a slightly better COD removal efficiency. The CEs of heliox and air reactors were almost the same.

Chapter 7

Future Work

This was the first study to apply heliox toward characterizing oxygen transport in MFCs systems. The performance of MFCs was successfully improved, with a reduction in the internal resistance of cathodes. However, there are still challenges to be addressed for further improvement, and the transport mechanisms need to be studied in more detail. Suggested future work on this subject is listed below:

1. The moisture in the gas-fed chambers should be removed. Obvious water drops were observed on the cathodes in this study, though the sparge gas went through desiccant to remove moisture and to keep comparable relative humidity.
2. The gas-fed chamber could be optimized to prevent uneven pressure. Different partial pressure across the cathode surface could nonuniformly impact oxygen diffusion.
3. It would be interesting to analyze the microbial communities and biomass accumulation on the cathodes and anodes of heliox-fed systems. Microbial communities at both electrodes can significantly influence the performance of MFCs, so characterization of these communities might allow a more complete interpretation of the mechanism of improvement caused by heliox.
4. The performance of heliox-acclimated MFCs could be studied after switching them from heliox to air. It might be interesting to see whether previously heliox-fed MFCs could sustain better performance due to the possible shift of

microbial community, or if they would revert to air-cathode performance due to the lower gas-phase oxygen transport.

5. Cathodes without Pt catalyst or with different support materials could be further studied in heliox-fed systems relate to an air-fed baseline.

References

1. EIA Annual Energy Review 2011. http://www.eia.gov/totalenergy/data/annual/pdf/aer.pdf

2. Logan, B. E., *Microbial fuel cells*. John Wiley & Sons: Hoboken, N.J, 2008.

3. McCarty, P. L.; Bae, J.; Kim, J., Domestic Wastewater Treatment as a Net Energy Producer-Can This be Achieved? *Environ Sci Technol* **2011,** *45*, (17), 7100-7106.

4. Logan, B. E.; Regan, J. M., Electricity-producing bacterial communities in microbial fuel cells. *Trends Microbiol* **2006,** *14*, (12), 512-518.

5. Rinaldi, A.; Mecheri, B.; Garavaglia, V.; Licoccia, S.; Di Nardo, P.; Traversa, E., Engineering materials and biology to boost performance of microbial fuel cells: a critical review. *Energ Environ Sci* **2008,** *1*, (4), 417-429.

6. Erable, B.; Feron, D.; Bergel, A., Microbial Catalysis of the Oxygen Reduction Reaction for Microbial Fuel Cells: A Review. *ChemSusChem* **2012,** *5*, (6), 975-987.

7. Rozendal, R. A.; Hamelers, H. V. M.; Buisman, C. J. N., Effects of membrane cation transport on pH and microbial fuel cell performance. *Environ Sci Technol* **2006,** *40*, (17), 5206-5211.

8. Guerrini, E.; Cristiani, P.; Trasatti, S. P. M., Relation of anodic and cathodic performance to pH variations in membraneless microbial fuel cells. *Int J Hydrogen Energ* **2013,** *38*, (1), 345-353.

9. Logan, B. E.; Hamelers, B.; Rozendal, R. A.; Schrorder, U.; Keller, J.; Freguia, S.; Aelterman, P.; Verstraete, W.; Rabaey, K., Microbial fuel cells: Methodology and technology. *Environ Sci Technol* **2006,** *40*, (17), 5181-5192.

10. Du, Z. W.; Li, H. R.; Gu, T. Y., A state of the art review on microbial fuel cells: A promising technology for wastewater treatment and bioenergy. *Biotechnol Adv* **2007,** *25*, (5), 464-482.

11. Oh, S.; Min, B.; Logan, B. E., Cathode performance as a factor in electricity generation in microbial fuel cells. *Environ Sci Technol* **2004,** *38*, (18), 4900-4904.

12. Harnisch, F.; Schroder, U., From MFC to MXC: chemical and biological cathodes and their potential for microbial bioelectrochemical systems. *Chem Soc Rev* **2010,** *39*, (11), 4433-4448.

13. Popat, S. C.; Ki, D.; Rittmann, B. E.; Torres, C. I., Importance of OH(-) transport from cathodes in microbial fuel cells. *ChemSusChem* **2012,** *5*, (6), 1071-9.

14. Juang, D. F.; Lee, C. H.; Hsueh, S. C.; Chou, H. Y., Power Generation Capabilities of Microbial Fuel Cells with Different Oxygen Supplies in the Cathodic Chamber. *Appl Biochem Biotech* **2012,** *167*, (4), 714-731.

15. Cha, J.; Choi, S.; Yu, H.; Kim, H.; Kim, C., Directly applicable microbial fuel cells in aeration tank for wastewater treatment. *Bioelectrochemistry* **2010,** *78*, (1), 72-79.

16. Cheng, S.; Liu, H.; Logan, B. E., Increased performance of single-chamber microbial fuel cells using an improved cathode structure. *Electrochem Commun* **2006,** *8*, (3), 489-494.

17. Santoro, C.; Agrios, A.; Pasaogullari, U.; Li, B. K., Effects of gas diffusion layer (GDL) and micro porous layer (MPL) on cathode performance in microbial fuel cells (MFCs). *Int J Hydrogen Energ* **2011,** *36*, (20), 13096-13104.

18. Zhang, F.; Saito, T.; Cheng, S. A.; Hickner, M. A.; Logan, B. E., Microbial Fuel Cell Cathodes With Poly(dimethylsiloxane) Diffusion Layers Constructed around Stainless Steel Mesh Current Collectors. *Environ Sci Technol* **2010,** *44*, (4), 1490-1495.

19. Zhang, F.; Cheng, S. A.; Pant, D.; Van Bogaert, G.; Logan, B. E., Power generation using an activated carbon and metal mesh cathode in a microbial fuel cell. *Electrochem Commun* **2009,** *11*, (11), 2177-2179.

20. Harnisch, F.; Wirth, S.; Schroder, U., Effects of substrate and metabolite crossover on the cathodic oxygen reduction reaction in microbial fuel cells: Platinum vs. iron(II) phthalocyanine based electrodes. *Electrochem Commun* **2009,** *11*, (11), 2253-2256.

21. Martin, E.; Tartakovsky, B.; Savadogo, O., Cathode materials evaluation in microbial fuel cells: A comparison of carbon, Mn2O3, Fe2O3 and platinum materials. *Electrochim Acta* **2011,** *58*, 58-66.

22. Erable, B.; Duteanu, N.; Kumar, S. M. S.; Feng, Y. J.; Ghangrekar, M. M.; Scott, K., Nitric acid activation of graphite granules to increase the performance of the non-catalyzed oxygen reduction reaction (ORR) for MFC applications. *Electrochem Commun* **2009,** *11*, (7), 1547-1549.

23. Zhao, F.; Harnisch, F.; Schroder, U.; Scholz, F.; Bogdanoff, P.; Herrmann, I., Application of pyrolysed iron(II) phthalocyanine and CoTMPP based oxygen reduction catalysts as cathode materials in microbial fuel cells. *Electrochem Commun* **2005,** *7*, (12), 1405-1410.

24. Liu, X. W.; Sun, X. F.; Huang, Y. X.; Sheng, G. P.; Zhou, K.; Zeng, R. J.; Dong, F.; Wang, S. G.; Xu, A. W.; Tong, Z. H.; Yu, H. Q., Nano-structured manganese oxide as

a cathodic catalyst for enhanced oxygen reduction in a microbial fuel cell fed with a synthetic wastewater. *Water Res* **2010,** *44*, (18), 5298-5305.

25. Matter, P. H.; Wang, E.; Arias, M.; Biddinger, E. J.; Ozkan, U. S., Oxygen reduction reaction activity and surface properties of nanostructured nitrogen-containing carbon. *J Mol Catal a-Chem* **2007,** *264*, (1-2), 73-81.

26. Kim, I. K.; Saville, A. L.; Sikes, K. L.; Corcoran, T. E., Heliox-driven albuterol nebulization for asthma exacerbations: An overview. *Respir Care* **2006,** *51*, (6), 613-618.

27. Lee, D. L.; Hsu, C. W.; Lee, H.; Chang, H. W.; Huang, Y. C. T., Beneficial effects of albuterol therapy driven by heliox versus by oxygen in severe asthma exacerbation. *Acad Emerg Med* **2005,** *12*, (9), 820-827.

28. Hess, D. R.; Fink, J. B.; T Venkataraman, S.; Kim, I. K.; Myers, T. R.; D Tano, B., The history and physics of heliox. *Respir Care* **2006,** *51*, (6), 608-612.

29. Herrera, O. E.; Wilkinson, D. P.; Merida, W., Anode and cathode overpotentials and temperature profiles in a PEMFC. *J Power Sources* **2012,** *198*, 132-142.

30. Srouji, A. K.; Zheng, L. J.; Dross, R.; Turhan, A.; Mench, M. M., Performance and mass transport in open metallic element architecture fuel cells at ultra-high current density. *J Power Sources* **2012,** *218*, 341-347.

31. Liu, H.; Logan, B. E., Electricity generation using an air-cathode single chamber microbial fuel cell in the presence and absence of a proton exchange membrane. *Environ Sci Technol* **2004,** *38*, (14), 4040-4046.

32. Feng, Y. J.; Yang, Q.; Wang, X.; Logan, B. E., Treatment of carbon fiber brush anodes for improving power generation in air-cathode microbial fuel cells. *J Power Sources* **2010,** *195*, (7), 1841-1844.

33. Zhang, F.; Merrill, M. D.; Tokash, J. C.; Saito, T.; Cheng, S.; Hickner, M. A.; Logan, B. E., Mesh optimization for microbial fuel cell cathodes constructed around stainless steel mesh current collectors. *J Power Sources* **2011,** *196*, (3), 1097-1102.

34. Ren, L. J.; Tokash, J. C.; Regan, J. M.; Logan, B. E., Current generation in microbial electrolysis cells with addition of amorphous ferric hydroxide, Tween 80, or DNA. *Int J Hydrogen Energ* **2012,** *37*, (22), 16943-16950.

35. Zhang, L.; Zhu, X.; Li, J.; Liao, Q.; Ye, D. D., Biofilm formation and electricity generation of a microbial fuel cell started up under different external resistances. *J Power Sources* **2011,** *196*, (15), 6029-6035.

36. *Standard Methods for the Examination of Water and Wastewater*. 21 st. ed ed.; American Public Health Association: New York, 2005.

37. Manohar, A. K.; Bretschger, O.; Nealson, K. H.; Mansfeld, F., The use of electrochemical impedance spectroscopy (EIS) in the evaluation of the electrochemical properties of a microbial fuel cell. *Bioelectrochemistry* **2008,** *72*, (2), 149-154.

38. He, Z.; Mansfeld, F., Exploring the use of electrochemical impedance spectroscopy (EIS) in microbial fuel cell studies. *Energ Environ Sci* **2009,** *2*, (2), 215-219.

39. Wei, B.; Tokash, J. C.; Zhang, F.; Kim, Y.; Logan, B. E., Electrochemical analysis of separators used in single-chamber, air-cathode microbial fuel cells. *Electrochim Acta* **2013,** *89*, 45-51.

40. Logan, B. E., *Environmental transport processes*. John Wiley & Sons: New York, 2008.